Nigerian Journal of Engineering, Technology, Science and Environment; 01 (2025): ISBN: 2493-4671
NIGERIAN JOURNAL OF ENGINEERING, TECHNOLOGY, SCIENCE AND ENVIRONMENT
Journal homepage: www.njetse.dsust.edu.ng

Modelling and Optimization of Hydraulic Production from Shea Butter Using RSM and ANFIS Approach

Allen, M.A.,[1] Umunna, M. F.,[3] Nwosu-Obieogu, K..,[2*] Nwogu, C.,[1] Okoye, J.,[4] Erokare, E.T.,[3] Okoh, P.C.,[5] Emumejaye, E. P[3]
[1]Department of Mechanical Engineering, Michael Okpara University of Agriculture, Umudike
[2]Department of Chemical Engineering, Michael Okpara University of Agriculture, Umudike.
[3] Department of Agricultural and Bio-system Engineering, Southern Delta University, Ozoro
[4] Department of Chemical Engineering, Enugu State University of Science and Technology, Enugu.
[5] Department of Civil and Water Resources Engineering, Southern Delta University, Ozoro

ARTICLE INFO
keywords:
Shea butter
RSM
ANFIS
Biohydraulics
Specific gravity

ABSTRACT
The study centered on the modeling and optimization of shea butter bio-hydraulic production utilizing Adaptive Neuro fuzzy Inference System (ANFIS) and Response Surface Methodology (RSM). The time and temperature were treated as independent variables, whereas the kinematic viscosity and specific gravity were regarded as dependent variables. The ANFIS-generated 3D plots clearly demonstrated that the process parameters exerted a substantial influence on the response. The Analysis of Variance (ANOVA) revealed that a second-order polynomial model with kinematic viscosity (R^2- 0.99, Adj R^2-0.98, Pred R^2-0.95) and specific gravity (R^2- 0.99, Adj R^2-0.99, Pred. R^2-0.99) exhibited a strong correlation between the actual and predicted responses. The kinematic viscosity of 45.71 mm^2/s and specific gravity of 0.88 were determined at a temperature of 36.83 ^oC and a duration of 1.368 hours. The gbell membership function (mf) achieved the lowest mean square error (MSE) of 0.019 for kinematic viscosity and 0.0007 for specific gravity compared to other membership functions after 500 epochs. This indicates a highly accurate predictive behaviour of the model. The ANFIS analysis yielded optimal results indicating that the kinematic viscosity and specific gravity were measured at a temperature of 40 ^oC and duration of 2 hours. The resulting hydraulic characteristics were found to be in accordance with the ASTM standards. The study's observations demonstrate that the ANFIS technique is a viable method for predicting the biohydraulic properties of shea butter. The characterizations of the shea butter oil were determined using FT-IR (Fourier Transform Infrared Spectroscopy) and GCMS (Gas Chromatography Mass Spectrometer). These analyses confirmed the successful production of the biohydraulics.

Corresponding Author: *Email address*: **kenenwosuobie@mouau.edu.ng (Allen** M.A**)**
Received 04 May 2025, Received in revised from 12 June 2025, Accepted 14 June 2025
Available Online 10-07- 2025
njetsefoe@gmail.com; njetsefoe@yahoo.com;

Please cite this article as: Allen et al. (2025). Modelling and Optimization of Hydraulic Production from Shea Butter Using RSM and ANFIS Approach .NJETSE, Vol. 1(01), (2025)

1. Introduction

The study involving the behavior of fluids when in motion is hydraulics; this applies to the flow of liquids in pipes, fluids contained in tanks, and other storage areas [1]. They are pressurized to generate mechanical power without the wear and tear of gears or levers [2]. They provide energy transmission through the system, which enables work and motion to be accomplished. They are also responsible for lubrication and heat transfer and are also essential in driving circuits, cylinders, drive systems, manifolds, and cylinders. Hydraulic oil plays an important role in the lubricating, cooling, and protection of the hydraulic system [2,3].

Researchers have been motivated to explore alternate possibilities to mineral oil-based hydraulic oil due to environmental issues [4, 5]. In certain open systems, hydraulic oil will unavoidably be discharged into the surrounding environment as a result of regular wear and tear, leakage and sputtering, accumulating inthe environment, leading to pollution [6]. Therefore, the strong interest in environmental sustainability has led to the adoption of organic oil for industrial fluids.Vegetable oil-based hydraulic oil is a type of lubricating oil that is environmentally beneficial. It is specifically hydraulic oil that uses vegetables as its basis oil. [4, 6]

Vegetable oils display excellent tribological properties such as lower friction coefficients than mineral oil-based fluids, lower evaporation, higher flash points, and viscosity index. Also, different additives are added to improve the oxidation inhibitors and pour point depressants of the oil [4, 7]. It exhibits good lubrication performance, oxidation resistance, temperature and hydrolysis stability, and biodegradability [8].

Vitteleria paradoxa (shear nut tree) is the tree that produces the shear nut and is an important source of vegetable fat in Africa. It naturally and often thrives throughout Africa, particularly in Cameroon, Senegal, Nigeria, Ivory Coast, and Ghana. Shea butter is primarily composed of triglycerides and unsaponifiable materials. It contains 40-55% fat per kernel. Other notable properties of Shea butter oil include high density, high viscosity, low volatility, and incompressibility. These characteristics make it well-suited for hydraulic formation [9, 10].

Researchers have documented the use of vegetable oils as hydraulic fluids in the machining sector. Xi et al. [11] developed a hydraulic fluid for metal cutting that is based on vegetable oil. This fluid effectively reduces cutting force, cutting temperature, and chip thickness, resulting in outstanding machining performance. Briggs and Victor [3] effectively assessed the appropriateness of groundnut oil as a

potential biohydraulic fluid. Menon and Rajasekara [12] effectively utilised Neem seed-derived plant-based lubricants in motorbike engines. The findings demonstrated that the oil is both environmentally friendly and biodegradable. Furthermore, the oil exhibited antiwear properties that were comparable to those of standard oil, as determined through engine performance analysis. Nwosu-obieogu et al. [9] state that glycerol, a byproduct of the transesterification process, is considered the primary raw material for biohydraulic production.

The pursuit of optimal operating conditions in hydraulic production has led to significant interest in modeling, prediction, and parameter optimization using techniques like Response Surface Methodology (RSM) and Adaptive Neuro-Fuzzy Inference System (ANFIS) [7]. RSM is particularly useful for evaluating linear, interaction, and quadratic effects of process variables to identify optimal operating conditions [13]. However, its applicability is constrained by the fact that the developed models are generally limited to the range of the experimental data and may not effectively capture complex, non-linear interactions among variables.

In contrast, soft computing approaches such as ANFIS have demonstrated superior predictive capabilities compared to traditional Artificial Neural Networks (ANN), owing to the integration of fuzzy logic, which enhances the learning and decision-making abilities of ANN models [9,14]. Several studies have successfully applied ANFIS in biodiesel production, including the work by Nassef et al. [15] on biodiesel synthesis from microalgae, Ogaga et al. [16] on *Thevetiaperuviana* seeds, and Betiku et al. [17] on the esterification of high free fatty acid palm kernel oil. Despite these advancements, there is a noticeable gap in the application of RSM and ANFIS for developing hydraulic fluids from shea butter. This study aims to address this gap by focusing on the production of biohydraulic fluid from shea butter oil.

2. Materials and Methods

2.1 Materials and Equipment

Shea butter used in this study was obtained from the National Research Institute, Umudike. The experimental setup included: a 250 mL three-neck flat-bottom flask, 500 mL round-bottom flask, glass beads, thermometers, plastic rod stirrers, a hot plate magnetic stirrer, 100 mL storage containers, a condensation unit, distillation unit, 50 mL burettes, funnels, 250 mL and 1 L conical flasks, 500 mL beakers, measuring cylinders (250, 500, and 1000 mL), a stopwatch, and 1 L separating funnels for phase separation.

2.2 Oil Characterization

The physicochemical properties of shea butter oil (SBO) were determined using ASTM standard

methods. Parameters measured included density, refractive index, moisture content, saponification value, viscosity, acid value, peroxide value, molecular weight, smoke point, ester value, and free fatty acid content. Functional group analysis and fatty acid profiling were carried out using Fourier Transform Infrared Spectroscopy (FTIR, Shimadzu FTIR-8400S) and Gas Chromatography-Mass Spectrometry (GC-MS), respectively [18, 19].

2.3 Acid-Catalyzed Esterification of Shea Butter

Following the procedure adapted from [7], the esterification process was conducted to reduce the free fatty acid content and improve the oil's thermal stability. A 500 g sample of shea butter was preheated at 60 °C for 10 minutes to ensure uniform melting. Methanol was added at a concentration of 60% w/w relative to the oil. Subsequently, concentrated sulfuric acid (15% w/w of the sample) was introduced as the catalyst. The reaction mixture was stirred at 55–60 °C using a magnetic hot plate for one hour in an open system. After the reaction, the mixture was transferred to a 500 mL separating funnel and left undisturbed for 24 hours to allow phase separation. Three distinct layers formed: the bottom layer containing impurities, the middle layer containing the esterified oil, and the top layer composed of excess methanol. The middle layer was isolated, washed with hot distilled water, and heated to 105 °C to remove residual moisture

2.4 Transesterification reactions (biodiesel production)

Biodiesel production from shea butter oil, was carried out bytransesterification of the shea butter with methanol. For each of the samples, 1000 mL (1 L) of oil was used. The sample was introduced into 2000 ml (2 L), 3 necks round bottom flask. A quick-fit reflux condenser will be fitted to the central neck of the flask. The reaction system, though an open one, is such that material (vapour) is not lost either as gas or vapour. This will be made possible by the reflux condenser, which circulates water within the column hence, condenses vapor back to the reaction chamber. Heating and stirring were achieved by the action of a magnetic heating plate with a stirring capsule. The reaction parameters (time, temperature, stirring speed, catalyst concentration, and mole ratio) were set as follows: time is 1 hour, temperature is 65 minutes, stirring or agitation speed is 400 revolutions per minute (rpm), catalyst (NaOH) concentration is 1% and alcohol and oil mole ratio is 6:1. After production, the biodiesel and glycerol mixture (with excess catalyst and methanol) were transferred into a separating funnel and left overnight. The crude glycerol from the bulk is separated through the tap

for purification before use for bio-hydraulic formulation.

2.5 Purification of crude glycerol

Glycerol was purified using the Briggs and Victor technique [3]. A quantity of 50 gof unrefined glycerol was subjected to heating at a temperature of 550^{o}C within a 250 ml container known as a beaker, which was positioned on a magnetic hot plate. The liquefied glycerol was made acidic by adding 1M sulphuric acid until it reached a pH of 4. The mixture was then moved into a separating funnel. The sample was incubated for duration of three hours to facilitate the formation of three different layers. The uppermost layer consists of a phase rich in fatty acids, the intermediate layer is composed of a phase abundant in glycerol, and the lowermost layer is an inorganic salt phase. The phase containing a high concentration of glycerol was gathered and neutralized with a 2M solution of potassium hydroxide. Subsequently, the water was evaporated at a temperature of 100°C. The glycerol produced was refined by a solvent extraction method using methanol as the solvent to encourage the separation of dissolved ions. A separation funnel was used to separate the precipitated salts. The purified glycerol is subjected to a drying process at a temperature of 70°C in order to eliminate any remaining methanol..

2.6 Biohydraulic formulation

In the production of bio-fluids, as described by [5], glycerol derived from the transesterification reaction between groundnut oil and methanol, in the presence of sodium hydroxide catalyst, was utilised as both the solvent and the main component. The blend consisted of 500 g of glycerol, which accounted for 90% of the total mass of the fluid blend. Glycerol, with a boiling point between 230-300 ^{o}C and a freezing point below -50 ^{0}C, can be used as an anti-freeze in automotive brake and clutch fluid formulations. It can be a substitute for polyoxyalkylene glycol ether blend, which has a boiling point of 200 ^{0}C and a freezing point of -10 ^{o}C.

2.7 Types of lubricants and additives employed and the formulation of biohydraulic fluid

In order to attain the desired characteristics of the brake and clutch fluid, various chemicals, including lubricants and additives, were added to the base substance in different proportions [5]. The lubricants and additives encompass the following:

2.7.1 Bio-butanol and methanol

Bio-butanol, commonly known as butyl alcohol, is a physiologically generated alcohol having a chemical formula of C_4H_9OH. It consists of four carbon atoms. It served as a solvent in the mixture. The substance

exhibits boiling and melting temperatures of 117.7 ^{0}C and -89.9 ^{0}C, respectively. Additionally, it possesses a viscosity of 2.573x10^{3}mPa at a temperature of 25 ^{0}C. In addition, it may dissolve in ethanol and methanol, which is why non-edible methanol is included in the lubricants used [5].

2.7.2 Diethylene glycol with furfural aldehyde

Diethylene glycol, a lubricant component, was used exclusively to decrease the freezing temperature of the fluid compound and enhance its formulation's freezing point characteristic. Additionally, an essential attribute of an acceptable brake fluid should offer a protective layer that safeguards the surface of these components from corrosion, even after the fluid has dissipated and disappeared from the automotive parts. Despite its corrosive nature towards iron and steel, diethylene glycol was used as both a diluent and retardant. Although this chemical is derived from fossils, the amount used in the entire recipe is so negligible that its contribution to emissions can be disregarded when compared to the desirable properties input in the overall formulation [5].

Graphite

Graphite is a substance that is effective at reducing friction between fluid molecules and the walls of a container. The addition of graphite dust dissolved in methanol served as a friction modifier, hence increasing the total viscosity index of the fluid. Graphite also functions as an anti-wear agent in the mixture [5].

2.7.3 Bitter leaf

Corrosion and rust inhibition, as well as antioxidant properties. Brake fluids commonly cause corrosion in the metal components they come into contact with, such as callipers, master cylinders, and ABS control valves. In order to prevent corrosion of the components they come into touch with, it is necessary for them to include additives such as corrosion inhibitors, as vapours may be produced during activities with extremely high temperatures. Certain leaves of the bitter leaf plant (*vernonia amygdalina)* have demonstrated the ability to effectively hinder the process of corrosion and rust formation in various materials. Additionally, it can function as an antioxidant. Consequently, dried leaves of bitter leaf plants were soaked in ethanol for a duration of two days, then filtered and combined with the base substance to achieve the desired inhibitory and antioxidant effects [5].

2.7.4 Monoethylene Glycol

Brake or clutch fluids should not freeze in the hoses or pipes, as this could cause them to fail in transmitting force. Brake fluids need to exhibit little compressibility, even when subjected to temperature variations. Depressing the brake pedal should result

in an equivalent amount of force being applied to the brake calliper piston. Fluid cooling is essential because when the operational temperature is extremely high, the fluid may reach its boiling point, leading to the introduction of moisture contaminants into the cooled fluid. To provide both antifreeze and coolant properties, a small amount of Monoethylene glycol lubricant, which is also soluble in most organic solvents, was used in the formulation recipe [5].

Table 1. Formulation of shea butter biohydraulic fluid

S/N	Chemical used	Function	Quantity (%)
1	Glycerol	Base chemical	90.00
2	Methanol	Formulation solvent	3.50
3	Diethyl glycol	Diluent and retardant	2.50
4	Graphite	Friction modifier, anti-wear	2.00
5	Bitter leaf powder	Corrosion inhibitor, antioxidant	0.30
6	Detergent	Detergent	0.20
7	Monoethylene Glycol	Anti-freeze, coolant	1.50

The glycerol obtained from shea butter transesterification was utilized as the base feedstock to produce biohydraulic coupled with other additives in various ratios listed in Table 1 to enhance its performance.

2.8 Experimental design

Central composite designimplementing response surface methodology was employed to model and optimize the process, In order to determine how the parameters affected biohydraulics, the two independent parameters; reaction temperature and time, were assessed. Table 2 displays the independent variables' levels and experimental range. The responses that were chosen were the specific gravity and kinematic viscosity, a total of 13 experiments was developed from the design [9].

Table 2: Summary of the experimental design for biohydraulic production

Factor	Units	Low level	Mid-level	High level
Time	Hour	1	2	3
Temperature	^{o}C	35	40	45

2.9 ANFIS Modelling Development

A MISO (multi-input single-output) fuzzy model is developed to estimate biohydraulic production using ANFIs [15,17]. This work utilised the Takagi-Sugeno fuzzy grid partitioning system to accurately model the non-linear variables. The ANFIs modelling process utilised three input variables (time (h) and temperature (^{O}C)) and two output variables (specific gravity and kinematic viscosity). This process was conducted using the fuzzy logic toolbox of MATLAB R2015b by Mathworks Inc., located in Natick, Ma, USA [20]. To enhance the efficiency of ANFIs, the data was normalized through min-max scaling. The ANFIS architecture consists of five layers, as depicted in Figure 3. Figure 3 depicts square nodes, referred to as adaptive nodes, which indicate that the parameters can be adjusted and learned. On the other hand, the circle nodes, known as fixed nodes,

represent parameters that have been picked. The rule set consists of two fuzzy if-then rules, which are commonly used.:

Rule 1: If x is A_1 and y isB_1, then f_1 =p_1 x + q_1x+r_1 (1)

Rule 2: If x is A_2 and y isB_2, then f_2 = p_2x +q_2x+r_2 (2)

Where A, B are linguistic terms that are user-defined and represent a range of values. The sequence and functions of the layers are as follows:

Layer 1: Square node equipped with node function

$O_i^L = \mu_{Ai}(x)$ (3)

Assuming x and y are the two typical input values fed at the two input nodes, transforming those values to the input membership functions. Where O_i^L is the membership function of A_i and x is the input parameter to the node. $A_i$is the linguistic label connected with the node function.

Layer 2: This node increases the homeward bound signal and releases the product out of the layer.w_i = $\mu_{Ai}(x) \times \mu_{Ai}(y),\ i = 1,2$ (4)

Layer 3: circle node. A node calculates the ratio of the i-th rule's firing strength to the sum of all rules' firing strengths:

$w_i^{'} = \frac{w_i}{w_1+w_2}\ , i = 1,2$ (5)

Layer 4: Square node with node function:

$O_i^4 = w_i^{'} f_i = w_i^{'}(p_i x + q_i y + r_i)$ (6)

p, q, r – parameter set (consequent, linear parameters)

Layer 5: circle node. This node computes the overall output as the summation of all incoming signals.

$O_i^5 = overalloutput = \sum_i w_i^{'} f = \frac{\sum_i w_i f_i}{\sum_i w_i}$ (7)

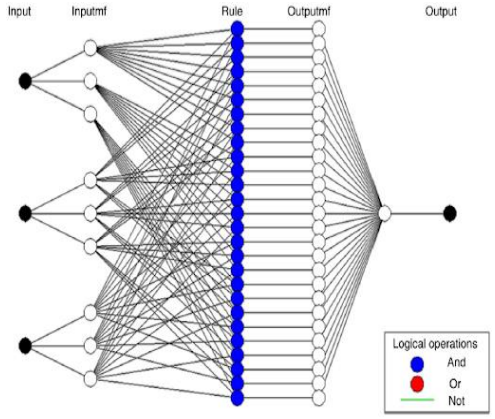

Fig 1: ANFIS basic structure

2.10 Developed Models Evaluation

The model's evaluation for the process was assessed using the statistical indicators below in equations 8 and 9

(Mean square error) MSE = $\frac{1}{P}\sum_{p=1}^{p}(d_p - O_p)^2$ (8)

(Coefficient of determination) $R^2 = 1 - \frac{\sum_{p=1}^{p}(d_p - O_p)^2}{\sum_{p=1}^{p}(O_p)^2}$ (9)

d_p and o_p represent the observed and the predicted values. The MSE value closeness to 0 and the R^2 value to 1 shows how well the model fits [21].

2.11 Biohydraulic characterization

Kinematic viscosity and specific gravity were used to evaluate the producedbiohydraulic and instrumentation such as FTIR (Shimadzu FTIR-8400S) was used to evaluate the functional group of the oil respectively [19, 22].

2.12 Kinematic viscosity at 40°C

The D445 Test Method was utilised to measure the kinematic viscosity of both transparent and opaque liquids, and to calculate the dynamic viscosity. A viscosity tube with a capacity of 861 units was partially filled with biodiesel, up to the halfway point of the bottom bulb. The tube was kept at a consistent temperature of 37.8° C for a duration of 30 minutes. Subsequently, the fluid was extracted from the upper bulb, and the duration of the fluid's discharge was measured. The duration of the flow was thereafter multiplied by the constant of the tube employed [23, 24].

2.13 Specific gravity determination

The specific gravity was obtained using the expression in Equation 10

$$specificgravity = \frac{weightofoil}{weightoftheequalvolumeofwater} \quad (10)$$

3. Results and discussion

3.1 Physicochemical properties of SBO

Table 3 presents the physicochemical characteristics of raw shea butter oil. The specific gravity (0.89) falls within the acceptable range for (International Standards Organization Viscosity Grade) ISOVG 32-grade hydraulic fluids (0.87–0.874), which is beneficial in minimizing microbial contamination. The oil exhibits high acid and free fatty acid (FFA) values of 4.38 mg KOH/g and 2.19%, respectively, suggesting limited hydrolytic degradation but indicating a potential risk of corrosion to soft metallic components in hydraulic systems [8,25]. Consequently, pretreatment is essential to reduce these values, thereby preventing soap formation and facilitating glycerol separation during processing.The measured saponification and peroxide values imply that the oil has good oxidative stability and is less susceptible to rancidity. With an iodine value of 70.8 g I_2/100 g, the oil demonstrates a moderate level of unsaturation. This is consistent with the findings of Briggs and Victor [3], who stated that oils with iodine values ranging between 60 and 128 are appropriate for hydraulic fluid applications. However, the oxidation stability of SBO was found to be below the ASTM D6751 standard of 3 hours, indicating the need for further treatment before use in biodiesel production. The stability observed might be influenced by the extraction method used, as noted in previous studies [27].The kinematic viscosity of the oil aligns closely with that of palm kernel oil (57.34 mm²/s), as reported by [16], supporting its potential as a viscous and effective feedstock for hydraulic applications. Additionally, the flash point of 157 °C reflects the oil's high thermal resistance and safety under elevated temperature conditions. The pour point of 10.89 °C suggests moderate flowability, indicating that the presence of

unsaturated triglycerides enhances both oxidation resistance and fluid behavior at lower temperatures

Table 3: Physicochemical properties of SBO

Physicochemical properties	SBO
Free fatty acid (FFA) (%)	2.19
Acid value (mgKOH/g)	4.38
Moisture content (%)	0.09
Saponification value (mgKOH/g)	106.17
Specific gravity	0.89
Kinematic viscosity at 40^{o}C (mm^{2}/s)	67.77
Molecular weight	744.30
Flash point	157
Peroxide value	5.95
Cloud point	12.56
Pour point	10.89
Oxidation stability 110^{o}C (Hour)	2.5
Refractive index	1.46
Iodine value (gI_2/100g)	70.85

3.2 Fatty Acid Composition of SBO

The fatty acid profile of shea butter oil was determined using Gas Chromatography-Mass Spectrometry (GC-MS), as presented in Table 4. The analysis revealed that oleic acid is the predominant fatty acid, comprising 55.5 wt%, followed by stearic acid at 21.81 wt%, myristic acid at 8.62 wt%, and linolenic acid at 6.82 wt%. Overall, the oil contains approximately 38.59 wt% saturated fatty acids and 62.32 wt% unsaturated fatty acids. This composition indicates that shea butter oil is rich in monounsaturated and polyunsaturated fatty acids, particularly oleic and linolenic acids, which are known to favor transesterification reactions. The high unsaturated fatty acid content supports the suitability of SBO for glycerol-based hydraulic fluid production, as these components enhance the oil's reactivity and performance characteristics [28, 29].

Table 4. Fatty acid profile of SBO for GCMS analysis

SBO	
Fatty Acid	Composition (%)
Capric acid	1.72
Lauric acid	-
Stearic acid	21.81
Palmitic acid	5.80
Myristic acid	8.62
Arachidic acid	0.64
Linolenic acid	6.82
Linoleic acid	-
Oleic acid	55.5
Total	100.91

3.3 Physiochemical properties of the produced biohydraulic

The physicochemical properties of the produced bio-hydraulic from SBO were compared with the conventional hydraulics, and the obtained results are presented in Table 5. Table 5 also showed how the produced bio-hydraulic was comparable to the conventional. The acid value (AV) shows the

specifications of oil, and it is determined as the weight of potassium hydroxide (KOH) in mg needed to neutralize the organic acid present in 1g [30]. AV also measures the breakdown of triacylglycerols into free fatty acids (FFA). The oxidation process increases the acid value and deteriorates the hydraulics. The AV results show that the oxidation effect affects the conventional hydraulic (8.69) more compared with the produced bio-hydraulic (2.09). The increase in the amount of FFA, as observed in the conventional hydraulic (4.35), indicates the hydrolysis of triglycerides. The FFA value for the produced bio-hydraulic (2.09) showed that the hydrolysis process of triglycerides was minimal. The hydrolysis of triglycerides was due to the action of the lipase enzyme, indicating a dysfunctional process condition [31].The observation from the FFA values revealed that the produced bio-hydraulic from SBO was better than the conventional. In a study conducted by Habib et al. [32], the free fatty acid content of orange seed oil was found to be 0.21 mg KOH/g oil, while mandarin seed oil had a free fatty acid content of 0.65 mg KOH/g oil. In a similar manner, [33] found that the acid value of orange seed oil extracted using n-hexane was 0.67 mg KOH/g oil, whereas the peroxide value was 6.37 meq 02 /kg oil. The refractive index (RI) is a crucial factor to consider while evaluating the appropriateness of oils. This is because greater refractive index (RI) values have a negative impact on the efficiency of oil. The RI values of the produced bio-hydraulic and conventional were comparable, with a difference of 0.0134, as shown in Table 5.The boiling point of the bio-hydraulic (333°C) and the conventional (345°C) were comparable to the boiling point of the biodiesel as reported by the US Department for Energy (2015); hence, high boiling point averts vaporization in the fluid pots and lines [5]. The smoke point of the produced bio-hydraulic and conventional also called the flash point, is the temperature at which the oil begins to break down into FFA [3]. The smoke point (106°C) valuecompared well with the conventional smoke point value. The cloud point shows that the conventional clouds or forms wax faster than the produced bio-hydraulic. The pour point, which is the lowest temperature at which the hydraulic losses its flow, indicates that the conventional hydraulic has good flow ability compared to the produced bio-hydraulic [3]; hence, there is a close agreement between the commercial and biohydraulic properties shown in Table 3

Table 5: Physiochemical properties of the produced biohydraulic

Sample	Biohydraulic	Commercial hydraulic
Acid value (mgKOH/kg)	4.18	8.69
Free fatty acid (mgKOH/kg)	2.09	4.35

Refractive index @ 29^{0}c	1.45	1.44
Boiling point (^{0}c)	333.00	345.00
Smoke point (^{0}c)	106.00	120.00
Cloud point	15.00	18.00
Pour point	4.50	7.00

3.4 FTIR of the extracted SBO

Figure 2 displays the FTIR spectrum of the SBO. The presence of functional groups in biohydraulic production indicates its suitability and efficiency [34]. The extracted SBO sample was analysed using an Agilent Technologies FTIR Spectrometer in the mid-infrared region, namely within the range of 3500 to 1000 cm^{-1}. The FTIR analysis indicated the presence of specific functional groups in the extracted SBO, including esters (C-D), alkene (CC), alkynes (CSC), alkanes (C-H), carbonyl (C-0), and alcohol (OH) bands [35]. The absorption spectrum of the SBO, as indicated by the band absorption at peak 3308.7-2922.2 cm^{-1}showingthe symmetric vibration of C-H alkane groups, demonstrates that it has low moisture content. This is evident in the physiochemical properties listed in Table 3.The absorption at 1625.1cm^{-1} corresponds to O-H and C=C group stretched in the carboxylic acid. The presence of carbonyl ester functional groups in the extracted SBO was confirmed by the characteristic peaks observed at 1244.4 during stretching vibrations. These bands are considered important when evaluating the suitability of extracted SBO as a viable substitute for bio-hydraulic production, as highlighted by [36], [37], and [34]. The absorption spectrum in the area of 1461.1-1379.1cm^{-1} exhibits bands that correspond to asymmetric and symmetric vibrations, indicating the presence of alkane (CH) and alkene (C) groups in the extracted 050. The FTIR analysis of SBO revealed that the region between 1237.5 and 1159.9 cm^{-1} was identified as containing esters and aromatic band functional groups, respectively. The out-of-plane bending vibrations at a frequency of 913.1cm^{-1} exhibited an alkene chain, as reported by [36].

3.5 FTIR of the Produced Bio-hydraulic

Figure 3 displays the results of the FTIR spectroscopic study, which was conducted to determine the functional groups contained in the bio-hydraulic fluid. The presence of functional groups yields valuable information and enhances the efficiency of the generated bio-hydraulic [34]. The bio-hydraulic sample was analysed using an Agilent Technologies FTIR Spectrometer, which scanned the sample within the mid-infrared region of 3500 to 1000 cm^{-1}. The FTIR study indicated that the bio-hydraulic now being generated possessed functional groups that exhibited the typical bands of esters (C=O), esters (C-O), Esther and Alkanes (C-H)

carbonyl (C-0), and hydroxyl (OH) [30,31,35]. The absorption spectrum of the band at peak 3224.8-2317.4 cm^{-1} indicates the existence of the OH hydroxyl group [38]. The absorption spectra at 2967.0, 2824.3cm^{-1}, and 1625.1 cm^{-1}, which correspond to symmetric stretching vibrations, serve as indicators of alkane and carbon bands. [34] Observed that these bands correspond to the vibrations of single and double bonds at low energy, suggesting the presence of functional groups known as olefins. The presence of carbonyl ester functional groups in the generated biohydraulic was confirmed by the distinctive peaks observed in the range of 13259-1408 cm^{-1} stretching [31]. When evaluating the suitability of bio-hydraulics as a viable alternative, the presence of functional groups exhibiting specific bands is taken into account [36]. In particular, the bands observed in the absorption spectrum at 1110.7cm^{-1}, which correspond to asymmetric and symmetric vibrations, indicate the presence of ether symmetric stretching groups in bio-hydraulics. The esters functional groups were identified in the FTIR analysis of bio-hydraulics at a

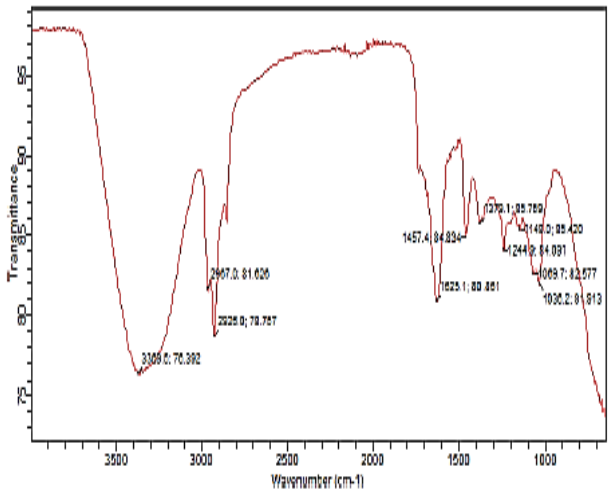

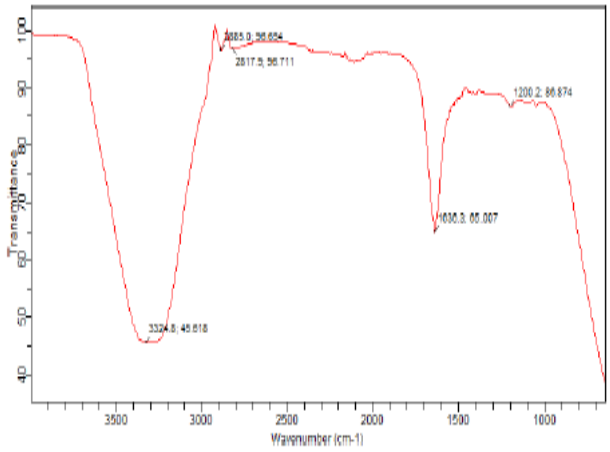

Fig. 3. FTIR of the sheabutter bio-hydraulic

3.6 Effect of process variation on biohydraulic yield

The general effect of temperature on the specific gravity and kinematic viscosity of the hydraulic is shown in Table 6. The hydraulic properties were compared with the conventional hydraulics. From the table, it was observed that an increase in temperature led to a non significant decrease in the specific gravity and the kinematic viscosity; this also was observed when compared to the commercial product; this agrees with the observation of Paredes et al.[39]; on the high pressure viscosity characterization of four vegetable and mineral hydraulic oils. Also, at a temperature of 35°C, the hydraulic kinematic viscosity of 44.89 was recorded, which was within

Nigerian Journal of Engineering, Technology, Science and Environment; 01 (2025): ISBN: 2493-4671
NIGERIAN JOURNAL OF ENGINEERING, TECHNOLOGY, SCIENCE AND ENVIRONMENT
Journal homepage: www.njetse.dsust.edu.ng

Table 7. RSM experimental run on the biohydraulic properties of shea butter

Run	time hrs	temperature Degree	kinematic viscosity	specific gravity
1	1	40	39.92	0.83
2	2	35	47.38	0.88
3	2	40	43.2	1.07
4	2	40	43.2	1.07
5	3	35	40.44	1.1
6	2	40	43.2	1.07
7	2	40	36.82	1.26
8	1	35	45.87	0.766
9	2	40	43.2	1.07
10	1	45	35.2	1.05
11	3	40	34.58	1.31
12	3	45	34.63	1.37
13	2	40	43.2	1.07

the standard (45.9); the same trend was replicated in the specific gravity of both the bio and the commercial hydraulic[3]. Hence, this shows that temperature has a significant effect on hydraulic properties; an increase in temperature leads to a rise in the kinetic energy of molecules and reduces the cohesive forces between the molecules of the liquid.

Table 6: Effect of process parameters on the biohydraulic yield

S/N	Temp. (^{0}C)	Bio-hydraulic Specific gravity	Commercial hydraulic specific gravity	Bio-hydraulic kinematic viscosity (mm^2s^{-1})	Commercial hydraulic kinematic viscosity (mm^2s^{-1})
1	25	1.219	1.0844	49.1655	24.9202
2	30	1.218	1.0840	47.4329	24.3796
3	35	1.217	1.0809	44.8919	23.1677
4	40	1.215	1.0766	40.1604	22.0589
5	45	1.213	1.0715	34.1021	19.1801
6	50	1.211	1.0651	30.1176	16.7467
7	55	1.205	1.0542	26.5549	13.0304
8	60	1.202	1.0423	18.6838	9.5542

$$\text{Kinematic viscosity} = 43.20 - 1.69A - 3.93B + 1.22AB - 3.14A^2 - 0.71B^2 \quad \textbf{(11)}$$

$$\textbf{Specific gravity} = \mathbf{1.07 + 0.1666A + 0.1363B - 0.1363AB + 0.0004A^2 + 0.0005B^2} \quad \textbf{(12)}$$

The data shown in Table 7 provides a comprehensive overview of the experimental results obtained from 13 different experiments conducted to measure the kinematic viscosity and specific gravity of the biohydraulics. These studies involved varying combinations of interacting variables. The experimental data underwent sophisticated multiple regression analysis to derive second-order polynomial equations with regression coefficients and were subsequently assessed for statistical significance. The results indicate that the variables had a substantial influence on the response [4]. In order to establish a correlation and create the model for the given data, a quadratic polynomial was used. The factors (A) time and (B) temperature have a relationship with the responses (kinematic viscosity and specific gravity). The coefficient of the quadratic polynomial regression model for the response described in equations 11 and 12 was determined using multiple regression approaches. The one-factor coefficient quantifies the impact of the specific variable. Conversely, the relationship between the

two variables and the quadratic effect is depicted by the two-factor and second-order coefficients. This aligns with the findings of [21] about the epoxidation of rubber seed oil using the combined approach of RSM and adaptive neuro-fuzzy inference system-genetic algorithm (ANFIS-GA).

Table 8: ANOVA for the model of kinematic viscosity of the biohydraulics

Source	Sum of Squares	df	Mean Square	F-value	p-value	
Model	221.23	5	44.25	218.27	< 0.0001	significant
A-time	22.96	1	22.96	113.25	< 0.0001	
B-temperature	123.36	1	123.36	608.53	< 0.0001	
AB	5.90	1	5.90	29.13	0.0010	
A^2	68.37	1	68.37	337.28	< 0.0001	
B^2	3.51	1	3.51	17.30	0.0042	
Residual	1.42	7	0.2027			
Lack of Fit	1.42	3	0.4730			
Pure Error	0.0000	4	0.0000			
Cor Total	222.65	12				
Std. Dev.	0.4502	R^2	0.9936			
Mean	40.83	Adjusted R^2	0.9891			
C.V. %	1.10	Predicted R^2	0.9547			
		Adeq Precision	41.8438			

Table 9: ANOVA for the model of specific gravity of the biohydraulics

Source	Sum of Squares	df	Mean Square	F-value	p-value	
Model	0.3706	5	0.0741	4281.82	< 0.0001	significant
A-time	0.2219	1	0.2219	12818.79	< 0.0001	
B-temperature	0.1487	1	0.1487	8587.63	< 0.0001	
AB	0.0000	1	0.0000	2.55	0.1540	
A^2	9.783E-07	1	9.783E-07	0.0565	0.0489	
B^2	1.409E-06	1	1.409E-06	0.0814	0.0137	
Residual	0.0001	7	0.0000			
Lack of Fit	0.0001	3	0.0000			

Pure Error	0.0000	4	0.0000
Cor Total	0.3707	12	
Std. Dev.	0.0042	**R^2**	0.9997
Mean	1.07	**Adjusted R^2**	0.9994
C.V. %	0.3887	**Predicted R^2**	0.9977
		Adeq Precision	214.2966

Table 8 presents the findings of the analysis of variance for kinematic viscosity. The model's R^2, adjusted R^2, and predicted R^2 were 0.9936, 0.9891, and 0.9547, respectively. These values indicate a strong fit for the model and a high correlation between the observed and expected values. The whole model demonstrated statistical significance (p-value <0.05). The single, interaction, and quadratic factors were found to be significant. The standard deviation (0.4502), coefficient of variation (C.V%) (1.10), and adequate precision (41.8438) suggest that the model is acceptable and resilient for optimising specific gravity. The values of R^2, adjusted R^2, and anticipated R^2 in Table 9 are all near to 1. The single and quadratic terms are significant, but the interaction term is not significant. This indicates that all the process factors had a significant impact on kinematic viscosity and specific gravity. The model is deemed appropriate and robust for optimisation based on the standard deviation (0.0042), coefficient of variation (C.V%) (0.3887), and adequate precision (214.2966). The results are consistent with the research conducted by [40] regarding the manufacture of biodiesel by the transesterification of shea butter oil, as well as the study by [41] which focused on optimising the two stages of biodiesel production using shea butter oil.

3.7: ANFIS simulation results

Table 10: ANFIS model efficiency for biohydraulic prediction from shea butter.

Input membership function	MSE (kinematic viscosity)	MSE (specific gravity)
Gauss	0.00267	0.01345
Dsig	0.02596	0.08564
Gauss2	0.03456	0.04663
Trap	0.09585	0.04968
Pi	0.02459	0.07549
Tri	0.0026	0.0245
Gbell	**0.0019**	**0.0007**
Psig	0.01456	0.0832

The ANFIS model was used to simulate the best forecast for shea butter biohydraulic production. This simulation involved several input membership functions, including gauss *mf*, gauss2 *mf*, gbell *mf*, tri *mf*, trap *mf*, psig *mf*, and dsig*mf*. The output membership functions were set with a constant 500 epoch number and a step size of 0.01. The mean square error (MSE) was utilised to assess the level of predictability of the models. Table 5 presents a summary of the ANFIS results for several input membership function types. The mean squared error

(MSE) values range from 0.00193251 to 0.08564. The lowest Mean Squared Error (MSE) values were achieved for kinematic viscosity (0.00193251) and specific gravity (0.00070017) at gbell*mf*, as seen in the table. Therefore, gbell mf provided the most accurate prediction for the process. The findings derived from this study exhibit a close resemblance and can be directly compared to a prior inquiry conducted by Nwosu-Obieogu et al. (2020) that employed ANFIS to simulate the process of extracting *huracrepitan* seed oil. Nevertheless, the tri mf exhibited the lowest mf. Nonetheless, the model successfully predicted the process [14,15].

3.8 Optimization of the process variables

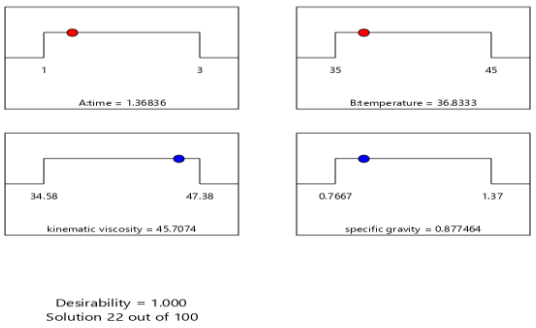

Fig. 4: Optimum Conditions ramp for biohydraulic production from shea butter

A numerical optimisation technique was employed to optimise the synthesis of shea butter biohyradulics, with the aim of determining the most favourable conditions for the process. Figure 4 shows that the optimal circumstances for the experiment were

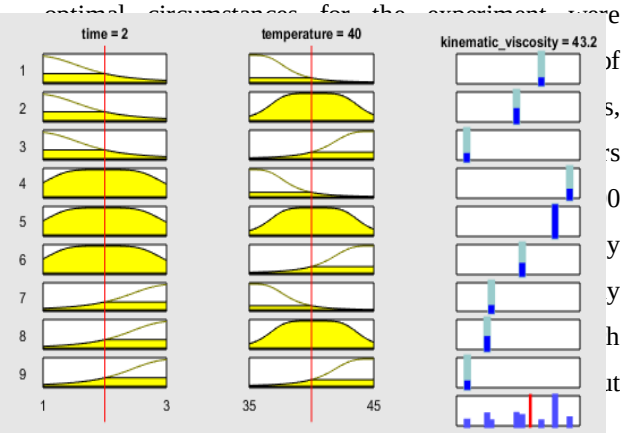

shell mercerization using the ANFIS technique, and by Oke et al. [21] on rubber seed oil epoxidation using RSM and ANFIS.

Fig. 5a: ANFIS surface plot for the kinematic viscosity of biohydraulic production from shea butter

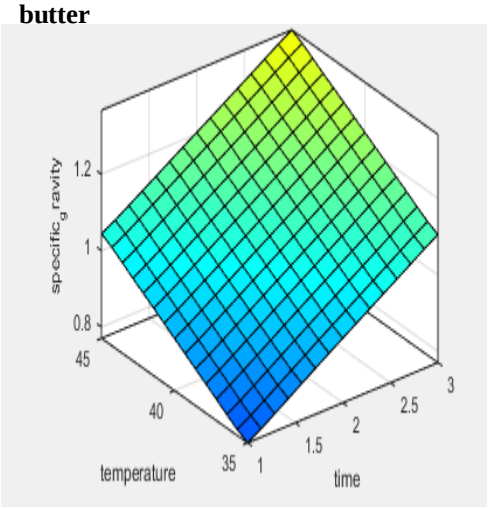

Fig. 5b: ANFIS surface plot for the specific gravity of biohydraulic production from shea butter

Fig. 6a: ANFIS rule viewer for the kinematic viscosity of biohydraulic production from shea butter

ANFIS surface plot for the kinematic viscosity and the specific gravity of biohydraulic from shea butter is presented in Fig. 5 and b. The kinematic viscosity and specific gravity were reduced when both time and time increased in the 3D model graph; this is a result of the increase in the randomness and collision of molecules, showing a significant impact of the independent parameters on the response. Also, the liquid contracts, making them denser. Hence, the behaviours depict that time and temperature impacted biohydraulic formation [20, 39]

Fig. 6b: ANFIS rule viewer for the specific gravity of biohydraulic production from shea butter

3.9 ANFIS Rule Analysis for Kinematic Viscosity and Specific Gravity

Figure 6a and 6b illustrate the ANFIS rule viewer for the kinematic viscosity and specific gravity in the biohydraulic production process. A key component of ANFIS is the fuzzy logic system, which governs how input parameters are mapped to output predictions. These rules can be adapted to predict outcomes even for untested input combinations, as long as they fall within the defined experimental domain. A total of nine fuzzy rules were employed to predict the kinematic viscosity and specific gravity. At a reaction time of 2 hours and a temperature of 40 °C, the model predicted a kinematic viscosity of 43.2 mm²/s and a specific gravity of 1.07. The close alignment between ANFIS and RSM outputs highlights the reliability and accuracy of the model in identifying optimal processing conditions [20, 21].

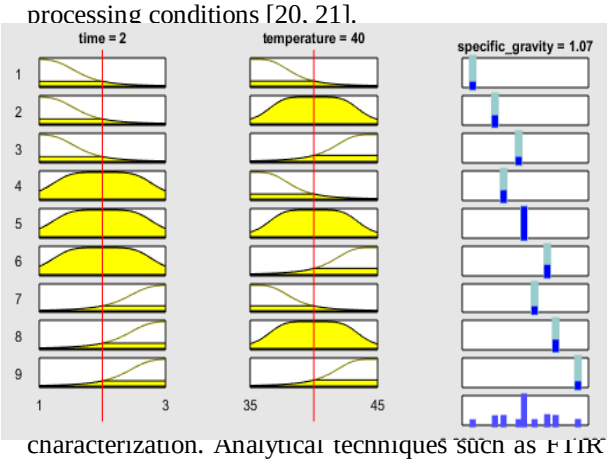

characterization. Analytical techniques such as FTIR and GC-MS confirmed the structural and compositional properties of the synthesized oil. The 3D surface plots and ANOVA results validated the

model's robustness and revealed that the process variables significantly influenced the response metrics. Among the membership functions tested, the generalized bell (gbellmf) function delivered the most accurate predictions, as evidenced by the lowest mean square error (MSE). The optimized results for kinematic viscosity and specific gravity, as predicted by both RSM and ANFIS models, met the ASTM specifications for hydraulic fluids. These insights also offer valuable implications for the efficient estimation of epoxides from AISO, supporting rapid and effective optimization of the epoxidation process using tools such as RSM and PSO.

Acknowledgment

The authors gratefully acknowledge the support provided by the Chemical Analysis Laboratory at the Department of Chemical Engineering, Michael Okpara University of Agriculture, Umudike, Abia State, Nigeria, for their instrumental role in the successful execution of this research

References

4. Paeglis, T., Karabeško, P., Mieriņa, I., Seržane, R., Strēle, M., Tupureina, V., & Jure, M. (2009). Compositions of hydraulic fluids based on rapeseed oil and its derivatives. In *8th International Scientific Conference: Engineering for Rural Development* (pp. 28–29).

5. Liu, X., Zhao, J., She, Y., & Liu, Y. (2023). Development history, current situation, and prospect of international vegetable oil-based hydraulic oil. In *E3S Web of Conferences*. EDP Sciences.

6. Briggs, T., & Victor, J. (2014). Determination of suitability of groundnut oil as a hydraulic fluid. *European Journal Of Mechanical Engineering Research*.

7. Callistus, N., Christopher, I., Kenechi, N. O., Patrick, C. N., Collins, N. O., Ndidi, F. A., &Nneka, E. C. (2023). *Uchenna optimization of dual transesterification of jatropha seed oil to lubricant using hybridized response surface methodology (rsm) and adaptive neuro-fuzzy inference system (ANFIS)-genetic algorithm (GA)*.

8. Eze, C. C., &Ezeribe, E. (2016). Formulation and Production of Bio-Hydraulic Fluid as an Alternative to Mineralfluids for Automobiles. *Am. J. Eng. Res*, *5*, 147–151.

9. Deuster , S., Schmitz, K., (2021)'Bio-based hydraulic fluids and the influence of hydraulic oil viscosity on the efficiency of mobile machinery', Sustainability, 13, (14), 7570.

10. Okechukwu, O. D., Joseph, E., Nonso, U. C., &Kenechi, N. O. (2022). Improving heterogeneous catalysis for biodiesel production process. *Cleaner Chemical Engineering*, 3–100038.

11. Pabsetti, P., Murty, R. S. V. N., Bhoje, J., Mathew, S., Rahul, K., &Feroskhan, M. (2023). Performance of hydraulic oils and its additives in fluid power system: A review. In *IOP Conference Series: Earth and Environmental Science*. IOP Publishing.

12. Nwosu-Obieogu, K., Onukwuli, D. O., Ezeugo, J., &Ude, C. N. (2023). Shea butter oil transesterification via clay doped barium chloride catalyst; response surface methodology and genetic algorithm evaluation. *Umudike Journal of Engineering and Technology*, *9*(1), 55–69.

13. P. A. Alaba, Y. M. Sani, I. Y. Mohammed, Y. A. Abakr, W. M. A. W. Daud, 'Synthesis and characterization of sulfated hierarchical nanoporousfaujasite zeolite for efficient transesterification of shea butter', J. Clean. Prod., (2017) 142, 1987–1993.

14. Xi, W., Kong, F., Yeo, J. C., Sonam, S., Dao, M., & Lim, C. T. (2017). Soft tubular microfluidics for 2D and 3D applications. *Proc. Natl. Acad. Sci. U. S. A*, *114*(40), 10590–10595.

15. Menon, K. S., &Rajasekaran, A. (2023). Evaluation of tribological properties and sustainability of bio-lubricant developed from neem seed oil for real-life application. *Tribol. Int*.

16. Marzouk, N. M., Naga, A. O. A., Younis, S. A., Shaban, S. A., El Torgoman, A. M., &Kady, F. Y. (2021). Process optimization of biodiesel production via esterification of oleic acid using sulfonated hierarchical mesoporous ZSM-5 as an efficient heterogeneous catalyst. *Journal of Environmental Chemical Engineering*, (2).

17. Okeleye, A. A., &Betiku, E. (2019). Kariya(Hildegardiabarteri) seed oil extraction : comparative evaluation of solvents , modeling , and optimization techniques. *Chemical Engineering Communications*, *7*(1), 1–18.

18. Nassef, A. M., Sayed, E. T., Rezk, H., Ali, M., Rodriguez, C., &Olabi, A. G. (2018). Environmental Effects Fuzzy-modeling with Particle Swarm Optimization for enhancing the production of biodiesel from Microalga Fuzzy-modeling with Particle Swarm Optimization for enhancing the production of biodiesel from Microalga. *Energy Sources, Part A: Recovery*, 1–10.

19. Ogaga, B., Adeleke, I. A., Damos, M., Adeola, H., Ernest, K., &Betiku, E. (2017). Optimization of biodiesel production from Thevetiaperuviana seed oil by adaptive neuro-fuzzy inference system coupled with genetic algorithm and response surface methodology. *Energy Conversion and Management*, *132*, 231–240.

20. Betiku, E., Odude, V. O., Ishola, N. B., Bamimore, A., Osunleke, A. S., &Okeleye, A. A. (2016). Predictive capability evaluation of RSM,

ANFIS and ANN: A case of reduction of high free fatty acid of palm kernel oil via esterification process. *Energy Convers. Manag*, *124*, 219–230.

21. Yatish, K. V., Prakash, R. M., Ningaraju, C., Sakar, M., Geethabalakrishna, R., &Lalithamba, H. S. (2021). Terminaliachebula as a novel green source for the synthesis of copper oxide nanoparticles and as feedstock for biodiesel production and its application on diesel engine. *Energy (Oxf.)*, *215*(119165).

22. Bambase, M. E., Almazan, R. A. R., Demafelis, R. B., Sobremisana, M. J., &Dizon, L. S. H. (2021). Biodiesel production from refined coconut oil using hydroxide-impregnated calcium oxide by cosolvent method. *Renew. Energy*, *163*, 571–578.

23. Nwosu-Obieogu, K. (2022). Modeling of Groundnut Shell Mercerization Process Using a Neuro-Fuzzy Technique. *Iranian Journal of Chemistry and Chemical Engineering*, *42*(4), 1320–1328.

24. Oke, E. O., Nwosu-Obieogu, K., Okolo, B. I., Adeyi, O., Omotoso, A. O., &Ude, C. U. (2021). Hevea brasiliensis oil epoxidation: hybrid genetic algorithm-neural fuzzy-Box-Behnken (GA-ANFIS-BB) modeling with sensitivity and uncertainty analyses. Multiscale and Multidisciplinary Modeling. *Experiments and Design*, *4*, 131–144.

25. Naveenkumar, R., &Baskar, G. (2020). Optimization and techno-economic analysis of biodiesel production from Calophylluminophyllum oil using heterogeneous nanocatalyst. *Bioresour. Technol*, *315*(123852).

26. Bhatia, S. K., Gurav, R., Choi, T. R., Kim, H. J., Yang, S. Y., Song, H. S., … Yang, Y. H. (2020). Conversion of waste cooking oil into biodiesel using heterogenous catalyst derived from cork biochar. *Bioresour. Technol*, *302*(122872).

27. Shimada, G. B., &Cestari, A. (2020). Synthesis of heterogeneous catalysts by the hydrolytic Sol-Gel method for the biodiesel production. *Renew. Energy*, *156*, 389–394.

28. Liu, Y., Ozbayoglu, E. M., Upchurch, E. R., &Baldino, S. (2023). Computational fluid dynamics simulations of Taylor bubbles rising in vertical and inclined concentric annuli. *Int. J. Multiph. Flow*, *159*(104333).

29. Sronsri, C., Sittipol, W., & U-Yen, K. (2021). Performance of CaO catalyst prepared from magnetic-derived $CaCO_3$ for biodiesel production. *Fuel (Lond.)*, *304*(121419).

30. Abnisa, F., .Sanni, S.E., andAlaba, P.A., (2021)‘Comparative study of catalytic performance and degradation kinetics of biodiesels produced using heterogeneous catalysts from kaolinite’, J. Environ. Chem. Eng., vol. 9, no. 4, p. 105569.

31. Qasemi, Z., Jafari, D., Jafari, K., &Esmaeili, H. (2022). Heterogeneous aluminum oxide/calcium

oxide catalyzed transesterification of*Mespilusgermanica*triglyceride for biodiesel production. *Environ. Prog. Sustain. Energy*, *41*(2).

32. Yu, H., Cao, Y., Li, H., Zhao, G., Zhang, X., Cheng, S., & Wei, W. (2021). An efficient heterogeneous acid catalyst derived from waste ginger straw for biodiesel production. *Renew. Energy*, *176*, 533–542.

33. Taufiq-Yap, Y. H., Lee, H. V., Hussein, M. Z., &Yunus, R. (2011). Calcium-based mixed oxide catalysts for methanolysis of Jatrophacurcas oil to biodiesel. *Biomass Bioenergy*, *35*(2), 827–834.

34. Weimin, L. I., Cheng, J. I. A. N. G., Xiaobo, W. A. N. G., &Weimin, L. I. U. (2015). Preparation and Tribological of Vegetable Oil Based Lubricating Oil Additive. *ActaPetroleiSinica (Petroleum Processing Section)*, *31*(2).

35. Habib, M. A., Hammam, M. A., Sakr, A. A., &Ashoush, Y. A. (1986). Chemical evaluation of egyptian citrus seeds as potential sources of vegetable oils. *J. Am. Oil Chem. Soc*, *63*(9), 1192–1196.

36. El-Adawy, T. A., El-Bedawy, A. A., Rahma, E. H., &Gafar, A. M. (1999). Properties of some citrus seeds. Part 3. Evaluation as a new source of protein and oil. *Nahrung*, *43*(6), 385–391.

37. Ezekoye, V., Adinde, R., Ezekoye, D., &Ofomatah, A. (2019). Syntheses and characterization of biodiesel from citrus sinensis seed oil. *Scientific African*, *6*(e00217).

38. Nwosu-Obieogu, K., Aguele, F., Chiemenem, L. I., (202) 'Soft computing prediction of oil extraction from huracrepitan seeds', Kem. U Ind., vol. 69, no. 11–12, pp. 653–658.

39. Adeniyi, A. G., Ighalo, J. O., &Onifade, D. V. (2020). Biochar from the thermochemical conversion of orange (citrus sinensis) peel and albedo: Product quality and potential applications. *Chem. Afr*, *3*(2), 439–448.

40. Bounaas, K., Bouzidi, N., Daghbouche, Y., Garrigues, S., De La Guardia, M., &Hattab, M. E. (2018). Essential oil counterfeit identification through middle infrared spectroscopy. *Microchem. J*, *139*, 347–356.

41. Borugadda, V. B., &Goud, V. V. (2014). Epoxidation of castor oil fatty acid methyl esters (COFAME) as a lubricant base stock using heterogeneous ion-exchange resin (IR-120) as a catalyst. *Energy Procedia*, *54*, 75–84.

42. Paredes, X., Comuñas, M. J., Pensado, A. S., Bazile, J. P., Boned, C., &Fernández, J. (2014). High-pressure viscosity characterization of four vegetable and mineral hydraulic oils. *Industrial Crops and Products*, *54*, 281–290.

43. Olatunji, O. M., Horsfall, I. T., &Ubom, E. V. (2021). Response surface optimization approach

to predict the maximum % biodiesel yield via transistor fi cation of esters fi edshea butter oil by utilizing. *Current Research in Green and Sustainable Chemistry*, *4*.

44. Ajala, E. O., Aberuagba, F., Olaniyan, A. M., Ajala, M. A., &Sunmonu, M. O. (2017). Optimization of a two-stage process for biodiesel production from shea butter using response surface methodology. *Egyptian Journal of Petroleum*, *26*(4), 943–955.

[8] Kemka, C., and Emeruwa, C. H. (2024). Temperature and Humidity Effect on Mobile Communication Network Performance in Yenagoa, Nigeria. *Nigerian Journal of Communications*, 40(1), 45–53.

[9] Akinwole, A. K., Olasunkanmi, O. S., and Ajani, O. O. (2023). Effect of Tropospheric Parameters on Received Signal Strength in GSM Networks in Rivers State, Nigeria. *International Journal of Wireless and Mobile Networks*, 15(1), 1–10. https://doi.org/10.5121/ijwmn.2023.15101

[10] Osahenvemwen, O., and Omatahunde, E. (2016). Effect of Weather Conditions on GSM Signal Strength in Benin City, Nigeria. *Nigerian Journal of Technology*, 35(3), 564–571.

[11] Boano, C., Brown, J., He, Z., Roedig, U., and Voigt, T. (2010). Low-power Radio Communication in Industrial Outdoor Deployments: The Impact of Weather Conditions and ATEX-compliance. *Sensor Applications, Experimentation, and Logistics*.

[12] OpenWeatherMap. (2021). Weather API Documentation. Retrieved from https://openweathermap.org/api

[13] Baig, M. S., Ismail, S. N., and Syed-Yusof, S. F. (2022). Machine Learning-Based TLS Analysis for Attack Detection in IoT Networks. *IEEE Access*, 10, 48731–48744.

[14] Abe, N., and Kudo, M. (2005**).** *Entropy criterion for classifier-independent feature selection*. In Proceedings of the 9th International Conference on Knowledge-Based Intelligent Information and Engineering Systems (KES 2005)**,** Lecture Notes in Computer Science, vol. 3684, pp. 905–911. Springer.